Hydrogen Production via a Commercially Ready

Inorganic membrane Reactor

Semi-Annual Technical Progress Report
Reporting Period: April 01, 2005 to September 30, 2005

Paul K. T. Liu
Project Director

August 23, 2005

Abstract

Single stage low-temperature-shift water-gas-shift (WGS-LTS) via a membrane reactor (MR) process was studied through both mathematical simulation and experimental verification in this quarter. Our proposed MR yields a reactor size that is 10 to >55% smaller than the comparable conventional reactor for a CO conversion of 80 to 90%. In addition, the CO contaminant level in the hydrogen produced via MR ranges from 1,000 to 4,000 ppm vs 40,000 to >70,000 ppm via the conventional reactor. The advantages of the reduced WGS reactor size and the reduced CO contaminant level provide an excellent opportunity for intensification of the hydrogen production process by the proposed MR. To prepare for the field test planned in Yr III, a significant number (i.e., 98) of full-scale membrane tubes have been produced with an on-spec ratio of >76% during this first production trial. In addition, an innovative full-scale membrane module has been designed, which can potentially deliver >20 to 30 m^2/module making it suitable for large-scale applications, such as power generation. Finally, we have verified our membrane performance and stability in a refinery pilot testing facility on a hydrocracker purge gas. No change in membrane performance was noted over the >100 hrs of testing conducted in the presence of >30% H_2S, >5,000 ppm NH_3 (estimated), and heavy hydrocarbons on the order of 25%. The high stability of these membranes opens the door for the use of our membrane in the WGS environment with significantly reduced pretreatment burden.

TABLE OF CONTENTS

List of Graphical Materials

Figures

List of Graphical Materials

Tables

1. Introduction

The advantage of using the low temperature shift (LTS) (vs the high temperature shift (HTS)) reactor is its high degree of conversion at this low temperature due to the exothermic reaction of WGS. In the conventional WGS process, HTS is performed as a first stage reactor to convert a majority of the CO, taking the advantage of the enhanced reaction kinetics at a high temperature (i.e., 350 – 450°C). Then the residual CO is sent to the LTS as a polishing step to reduce CO to the level of =1%. Based upon the enhanced efficiency delivered by the MR via the in-situ removal of the reaction products, it is possible to achieve the CO conversion nearly completely via the single stage, LTS. Thus, the process intensification objective can be fulfilled since (i) the HTS reactor is no longer needed, and (ii) the enhanced LTS is sufficient for CO conversion. For our present study, we focus on the use of the conventional Cu/Zn-based catalyst. Other catalysts, such as sulfide-based, will be investigated in the 2nd half of this project.

A mathematical model has been developed to predict the performance of the proposed membrane reactor for water gas shift reaction (WGS), so that the operating conditions can be optimized. In addition, a mathematical model can guide us to tailor a suitable membrane, in terms of permeance and selectivity, to commensurate with the existing commercial catalyst performance. Oxygen blown gasifier off-gas was used as an example in this study. In addition to the material balance check performed in Sec. 1, the prediction from the mathematical model was compared with the experimental results to validate the model prediction.

To prepare for the field test planned for Yr III at the PFDU, we have been actively pursuing the manufacturing of the full size membrane element (30"L) and the conceptual design of the full-scale module. This production run would produce enough inventory for the membrane requirement for the field test. More importantly, based upon the on-spec ratio of the full-scale membrane production run, the product cost can be estimated realistically.

This semi-annual report summarizes our activities in the above areas.

2. Executive Summary

Single stage low-temperature-shift water-gas-shift (WGS-LTS) via a membrane reactor (MR) process was studied through both mathematical simulation and experimental verification in this quarter. Using the kinetic parameters experimentally obtained by us, we are able to validate the mathematical model via the bench-top experimental results. Although the thermodynamic conversion of CO could be as high as ~90% in the LTS range, our proposed MR yields a reactor size that is 10 to >55% smaller than the comparable conventional reactor for a CO conversion of 80 to 90%. In addition, the CO contaminant level in the hydrogen produced via MR ranges from 1,000 to 4,000 ppm vs 40,000 to >70,000 ppm via the conventional reactor. The advantages of the reduced

WGS reactor size and the reduced CO contaminant level provide an excellent opportunity for intensification of the hydrogen production process by the proposed MR

To prepare for the field test planned in Yr III at the PFDU facility, we have focused in this quarter on (i) full-scale membrane production, (ii) full scale membrane module design and fabrication, (iii) membrane performance stability testing under harsh field environment, (iv) thermal management, and (iv) assessment of the benefit of using our proposed MR at the PFDU facility. A significant number (i.e., 98) of full-scale membrane tubes have been produced with an on-spec ratio of >76% during this first production trial. An innovative full-scale membrane module has been designed, which can potentially deliver >20 to 30 m^2/module making it suitable for large-scale applications, such as power generation. Finally, we have verified our membrane performance and stability in a refinery pilot testing facility on a hydrocracker purge gas. No change in membrane performance was noted over the >100 hrs of testing conducted in the presence of >30% H_2S, >5,000 ppm NH_3 (estimated), and heavy hydrocarbons on the order of 25%. The high stability of these membranes opens the door for the use of our membrane in the WGS environment with significantly reduced pretreatment burden. The activities on (i) reducing the pretreatment requirement and (ii) improving the WGS efficiency at the PFDU facility are continuing; their results will be reported in the next semi-annual report.

3. Experimental

3.1. *Mathematical Model, Kinetic Parameters and Feed Composition.*

3.1.1. Mathematical Model and Kinetic Parameters

A mathematical model can be developed based upon the material balance coupled with the reaction rate equations. The model, once developed, can then be solved numerically via the finite difference method. A steady state condition with concentration profile along the axial direction of the reactor is assumed here.

3.1.2. Feed Composition.

The feed composition is represented by $CO:H_2:CO_2:H_2O = 1.00:0.70:0.33:1.10$. The water content was calculated based upon 1.1 times of the stoichiometric requirement for the complete conversion of CO present. This H_2O to CO ratio, i.e., 1.1, is deemed to be minimal requirement for WGS. According to our calculations, assuming that the off-gas is available at ~1,200°C, quenching the reaction with water to the 1.1:1 ratio would yield a stream temperature of ~600°C. Hence, additional cooling is necessary to chill the stream to the LTS range of ~200°C and can be accomplished via indirect cooling. The indirect cooling allows one to recover the heat for other purposes. The advantage of the indirect cooling at a lower temperature is the use of less exotic heat exchanger material. From the reaction kinetic standpoint, the use of the minimum steam: CO ratio here is

justified versus 3:1 in the conventional reactor, since the improved efficiency of the proposed MR compensates for the rate loss.

3.2.   *Comparison of Packed Fixed-bed Reactor (PFR) vs Membrane Reactor (MR) for WGS-LTS (based upon simulation).*

The equilibrium conversion of CO for the LTS reaction is very high. For instance, about 89.9% conversion at 250°C with the composition of $CO:H_2:CO_2:H2O = 1:0.70:0.33:1.1$. Thus, instead of the comparison of the conversion levels in our study the comparison was made as follows:

Demonstrate the enhanced reaction rate at LTS with the use of the MR. W/F (gm cata
- lyst/g mol CO/hr) was used as a parameter to determine the %CO conversion as a function of W/F. Essentially the reactor size requirement to reach a given level of CO conversion is compared between MR and PFR.
- Determine the hydrogen purity of the product produced from MR vs PFR.

3.3.   *Experimental Verification of Mathematical Model*

The mathematical model developed was verified by experimental study performed in a laboratory scale membrane reactor. The experiment was held at 250°C and $P_{feed} = 3$ bar and $P_{perm} = 1$ bar. Feed Composition selected is $H_2:H_2O:CO:CO_2 = 4:1.1:1:0.01$. The CO conversions at the exit of both feed and permeate sides were measured to verify the mathematical model prediction.

3.4.   *Full Scale Membrane and Module Production*

The full-scale membranes were prepared according to the protocol we developed previously. Once prepared, the membrane permeances were determined at 120°C for its He, H_2, and N_2 permeance. Nitrogen was used as a surrogate gas for CO. In addition, we packaged the individual tubes together as a bundle using ceramic potting material. The bundle will then be used for future field test.

3.5.   *Simulation of WGS Under Field Operating Condition*

Our simulation shown in Sec. 3.3 demonstrates the advantages of a membrane reactor under a bench-top operating condition. Further, the simulation was experimentally verified at the condition which can be easily accomplished in our existing laboratory environment. In this section, we attempted to simulate the process close to the field operating condition; thus, the anticipated improvement via the use of the proposed membrane reactor can be quantified. Details of the simulation parameters are presented below:

*Permeate Side Purge Ratio...*In the field operation, some purging of the permeate side can provide enhanced membrane productivity, particularly if steam generated from low quality waste heat is used. Thus, our first task in this section is to evaluate the effect of

purge flow rate. Although the purge is accomplished by low pressure gas stream, from the cost minimization standpoint, it is beneficial to minimize the purge rate. Our simulation selected purge rates of 10 to 40% of the feed rate to study the effect on CO conversion.

*Reactor Pressure...*In our simulation of a lab scale reactor, the feed side pressure was kept low at about 3 to 5 bar. The actual gasifier off-gas could deliver 30 to 80 bar pressure or even higher. Thus, the effect of pressure on the CO conversion and the contaminant level is a critical aspect of our simulation of the field scale reactor. In this report, we study the operation at a much higher pressure, i.e., 15 and 3 bar feed and permeate side pressures, respectively.

*Permeance and Selectivity...*Also our membrane manufacturing development has made significant progress recently as detailed in Sec. 5. Based upon the performance data on these full scale membranes, H_2 permeance = 4 m^3/m^2/hr/bar at 250°C (projected from the data at 120°C shown in Figure 5) and H_2/CO = 100 appears achievable. Thus, these performance data were used in our simulation in this section.

*Field Test Under Harsh Environment...*While we are currently working on the opportunity to test the WGS from coal based utility plant in Yr III, the membrane developed from this project was field tested at ChevronTexaco's refinery pilot test facility for hydrogen recovery from a refinery waste stream (hydrocracker purge gas). More importantly this test stream provided an opportunity to evaluate the membrane stability operated under a harsh industrial environment, such as the presence of sulfur, ammonia and heavy hydrocarbons, which are commonly encountered in coal gasification applications.

*Membrane Challenge Test...*Finally our hydrogen selective membrane was subject to a challenge test at the end of this field test. The membrane was exposed to dead-end gas separation (i.e., exposed to the enriched contaminants) for about 17 hours in the field. The permeance was recorded before the challenge test, at the end of the dead-end test, and after the regeneration to determine the degree of permeance poison and its restoration.

4. Results and Discussion

4.1. *Mathematical Model, Kinetic Parameters and Feed Composition*

The mathematical model (see Appendix I) has been developed during this reporting period. To verify its accuracy, a material balance check was performed numerically. The results presented in Appendix II validate the model. This model, along with the kinetic parameters obtained experimentally, has been employed for comparison between the packed bed and the proposed membrane reactor for a single stage WGS-LTS reaction.

For all the calculations performed here we utilized the kinetic equations for WGS, described as follows [Ref. 1.]

$$r = A \cdot \exp(-E_a / RT) \cdot \frac{P_{CO} \cdot P_{H_2O}^{1.4}}{P_{CO_2}^{0.7} \cdot P_{H_2}^{0.9}} \frac{1}{P_t^{0.4}} (1 - b)$$

$$b = \frac{1}{K_g} \frac{(P_{CO_2} \cdot P_{H_2})}{(P_{CO} \cdot P_{H_2O})}$$

$$K_g = \frac{P_{CO_2} \cdot P_{H_2}}{P_{CO} \cdot P_{H_2O}}$$

A is the preexponential factor, E_a is the apparent activation energy, P_i is the partial pressure of component i, P_t is the total pressure, β is the approach to equilibrium, and K_g is the equilibrium constant for the water-gas shift reaction. The activation energy, E_a, listed in the reference is $E_a = 86.5$ (kJ/mol). The experimental E_a obtained by our study during this period is $E_a = 114.2$ (kJ/mol). Details of the experimental results are listed in Table 1 and Figure 1 below. The preexponental factor, A, obtained based upon our experimental E_a is $A = 1.77 \times 10^{11}$ (mol/g-hr-bar$^{0.4}$)

# Table 1.   Experimental Results for Kinetic Parameter Determination

Composition	CO : H2 : H2O = 1.0 : 4.0 : 2.5					
Pressure(psig)	52.5		50		50	
Temperature(C)	205		225		250	
Weight of Catalyst(g)	10		30		30	
	W/Fo CO (g*hr/mol)	CO Conversion(%)	W/Fo CO (g*hr/mol)	CO Conversion(%)	W/Fo CO (g*hr/mol)	CO Conversion(%)
	1.56E+02	77.96	4.67E+02	96.52	4.67E+02	96.63
	7.78E+01	68.47	2.33E+02	95.23	2.33E+02	95.21
Kinetic data	5.19E+01	61.66	1.56E+02	92.22	1.56E+02	92.94
	3.89E+01	50.93	1.17E+02	88.19	1.17E+02	88.43
	3.11E+01	47.96	9.33E+01	79.38	9.33E+01	86.35
	2.59E+01	38.48	7.78E+01	71.78	7.78E+01	77.86
Equilibrium Conversion of CO(%)	98.30		97.54		96.27	

$k = k_o \exp(-E/RT)$			
T(C)	205	225	250
T(K)	478.15	498.15	523.15
R(J/ mol*K)	8.314	8.314	8.314
k	5.39E-02	2.21E-01	6.46E-01

ln (k)	-2.92E+00	-1.51E+00	-4.37E-01
1/RT	2.52E-04	2.41E-04	2.30E-04

intercept (= ln (ko))	25.90
slope (= -E)	-114218.6

ko g-mol/(g cat*hr*bar^0.4)	1.77E+11
E (J/mol)	114218.6
E (KJ/mol)	114.22

intercept = ln(ko) = 25.90
slope = - E = - 114218.6
r ©÷ = 0.9864029922
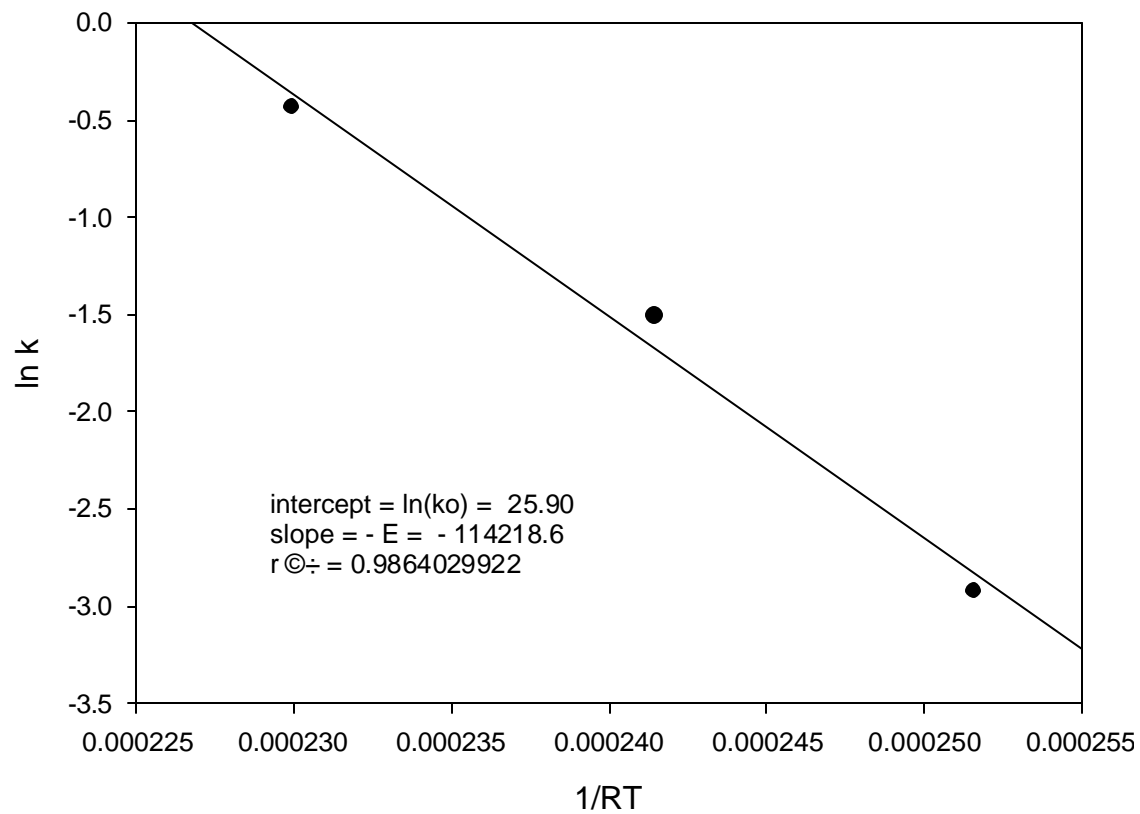
ln(k) vs. 1/RT

Figure 1   Experimental determination of Ea and A based upon ln(k) vs. 1/RT

The kinetic parameters, obtained for the Sud-Chemie catalyst used in this study, are different from that reported in the literature as shown above. As expected the MR performance predictions used ours vs the literature's are significantly different. However, the performance trend and the comparative difference between the membrane reactor (MR) and the packed fixed-bed reactor (PFC) are quite similar as shown in Table 2. Throughout this study, we employed the kinetic parameters obtained from our experimental study. It is believed that the conclusions generated with our own kinetic parameters would be applicable to other cases.

Table 2   Membrane Reactor Performance Prediction based upon Ours vs. Literature Kinetic Parameters

Case A. Using the kinetic parameters from the literature
k = 1.52 E8 (gmole/(gr catal.hr.bar^0.4)
Ea = 86500 (J/mol)

Xe	PFR	W/FCO(g*hr/mol CO) required to reach 95% of equilibrium conversion at PFR					
		1X H2		5X H2		10X H2	
		MR-co	MR-counter	MR-co	MR-counter	MR-co	MR-counter
0.899	34.0	26.0	32.4	18.2	20.1	14.2	14.7

Xe	PFR	W/FCO(g*hr/mol CO) required to reach 90% of equilibrium conversion at PFR					
		1X H2		5X H2		10X H2	
		MR-co	MR-counter	MR-co	MR-counter	MR-co	MR-counter
0.899	19.5	16.9	18.7	12.8	14.1	10.4	11.1

Case B. Using the kinetic parameter we obtained experimentally
k= 1.77 E11 (gmole/(gr catal.hr.bar^0.4)
Ea = 114218.6 (J/mol)

Xe	PFR	W/FCO(g*hr/mol CO) required to reach 95% of equilibrium conversion at PFR					
		1X H2		5X H2		10X H2	
		MR-co	MR-counter	MR-co	MR-counter	MR-co	MR-counter
0.899	23.6	17.5	19.9	13.0	14.2	10.2	10.7

Xe	PFR	W/FCO(g*hr/mol CO) required to reach 90% of equilibrium conversion at PFR					
		1X H2		5X H2		10X H2	
		MR-co	MR-counter	MR-co	MR-counter	MR-co	MR-counter
0.899	12.9	11.2	11.8	9	9.7	7.5	7.9

4.2.   Comparison of Packed Fixed-bed Reactor (PFR) vs Membrane Reactor (MR) for WGS-LTS (based upon simulation).

The CO conversion (%) vs W/F ranging from 10 to 60 was analyzed and is shown in Figure 2. In addition, three catalyst loading levels were chosen for our laboratory scale MR reactor, 10, 20 and 30 gm as shown in the same figure. Table 1 lists the W/F required to reach a given level of conversion for PFR and MR including both counter- and co-current operations. In addition, three different levels of hydrogen permeances were selected to display their effect on conversion. Key findings include:

- For the case using our own reaction kinetic parameters, the MR shows a ~10 to 40% reduction in reactor size over the PFR to reach 90% of the equilibrium conversion (89.9%). A more dramatic reduction of 25 to 55% in the reactor size was realized at 95% of the equilibrium conversion. As is evident, as the conversion approaches the equilibrium conversion, the PFR becomes very inefficient in comparison with the MR.
- For the MR operation, the amount of the catalyst usage within the range of our study, i.e., 10 to 30 gm, shows very minor effect on the conversion level for a given W/F.

- For MR, the performance of the co-current operation is similar to that of the counter-current operation. However, when the catalyst dosage or the flow rate is low (e.g., W=10g, or Fco=1X) and the required conversion level is ~ 80%, the co-current operation requires less W/F than the counter-current operation. Although this may seem counter-intuitive, it appears, based upon the simulation results, that the loss of CO at the feed end of the reactor to the permeate is higher in the counter current case. Since this CO is now unavailable for reaction, the conversion is reduced.
- A CO concentration of 1,000 to 4,000 ppm in the hydrogen product can be achieved in an MR. This contaminant level is much lower than that delivered by the PFR of 40,000 to >70,000 ppm. The much-reduced CO achieved with the MR results from the higher level of conversion and the in-situ product separation delivered by the membrane.

In summary, our mathematical simulation for the single stage LTS-WGS operation with MR demonstrates its unique advantage in achieving high CO conversion in a reactor volume that is 10 to >55% less than the PFR requirement. In addition, the CO level is low at 1,000 to 4,000 ppm and can be readily post-treated with existing polishing technologies, such as PROX or methanation. In comparison, the PFR cannot deliver the CO contaminant at a level low enough for further treatment by the PROX or methanation; an additional unit operation to separate CO contaminant from hydrogen is necessary.

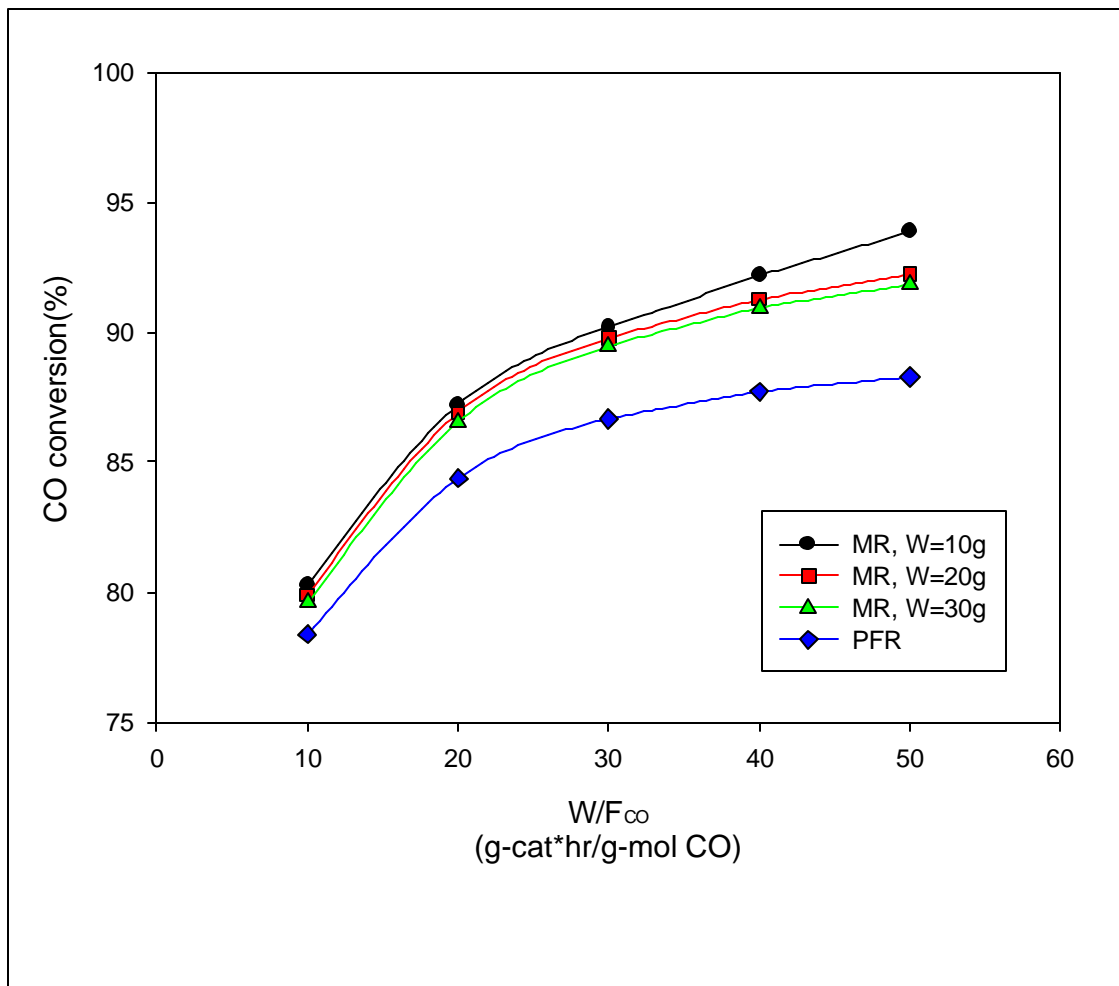**Figure 2** **CO conversion (%) with membrane reactor (MR) and packed fixed-bed reactor (PFR): varying the molar flow rate at the fixed W.**
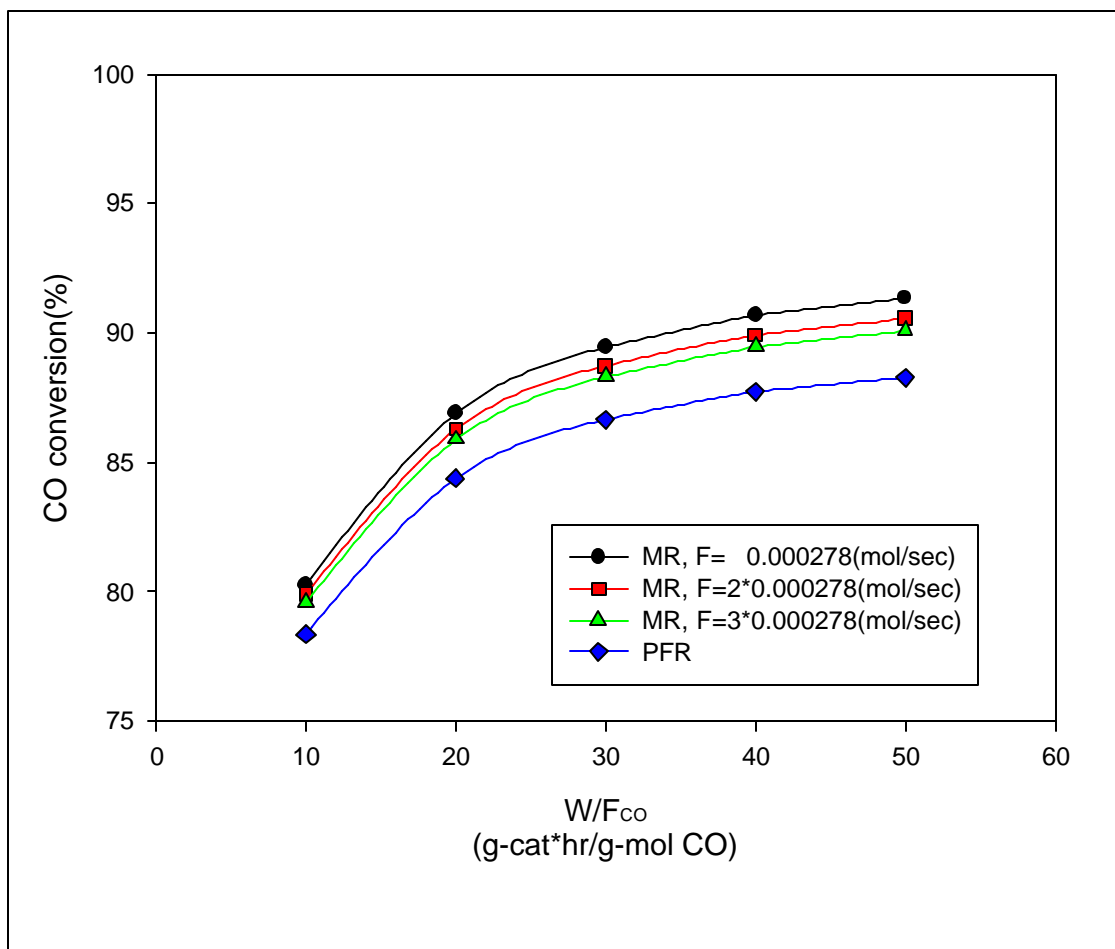
Figure 3   **CO conversion vs W/F$_{co}$ for MR and PFR: varying the amount of catalyst at the fixed F$_{co}$.**

Table 3   CO contaminant levels in the hydrogen products produced from PFR and MR with co- and count-current operation.

Coal gasifier-off gas composition(Oxygen blown)
T= 250
PF = 5 atm, PP = 1 atm
Sweep gas ratio = 0.1
Rich's case

Fixed W=10(g)								
	PFR		MR-co			MR-counter		
W/F	X	CO(ppm)	X	CO(ppm)	Re	X	CO(ppm)	Re
10	78.4	76777.0	80.3	3717.2	31.8	78.1	4007.8	31.9
20	84.4	54271.0	87.2	3064.7	55.8	83.6	3687.8	56.8
30	86.7	45999.0	90.2	2909.7	73.6	86.9	3936.9	75.1
40	87.7	42156.0	92.2	2958.4	85.1	90.5	4483.9	86.4
50	88.3	40195.0	93.9	3107.6	91.8	93.8	5271.1	92.2

Fixed W=20(g)								
	PFR		MR-co			MR-counter		
W/F	X	CO(ppm)	X	CO(ppm)	Re	X	CO(ppm)	Re
10	78.4	76774.0	79.9	3337.2	17.5	78.9	3462.0	17.4
20	84.4	54271.0	86.9	2567.1	32.2	85.0	2814.7	32.4
30	86.7	45999.0	89.8	2243.8	45.2	87.5	2616.2	45.8
40	87.7	42155.0	91.3	2085.7	56.6	89.0	2583.5	57.6
50	88.3	40195.0	92.2	2015.4	66.3	90.5	2641.1	67.7

Fixed W=30(g)								
	PFR		MR-co			MR-counter		
W/F	X	CO(ppm)	X	CO(ppm)	Re	X	CO(ppm)	Re
10	78.4	76774.0	79.6	3196.5	12.2	79.0	3272.9	12.1
20	84.4	54271.0	86.6	2411.9	22.8	85.3	2560.5	22.9
30	86.7	45999.0	89.4	2067.5	32.5	87.8	2288.6	32.8
40	87.7	42155.0	90.9	1878.4	41.4	89.2	2168.9	41.9
50	88.3	40195.0	91.8	1768.2	49.6	90.2	2125.0	50.4

Fixed Fco=0.00027778[mol/sec]								
	PFR		MR-co			MR-counter		
W/F	X	CO(ppm)	X	CO(ppm)	Re	X	CO(ppm)	Re
10	78.4	76774.0	80.3	3717.2	31.8	78.1	4007.8	31.9
20	84.4	54271.0	86.9	2567.1	32.2	85.0	2814.7	32.4
30	86.7	45999.0	89.4	2067.5	32.5	87.8	2288.6	32.8
40	87.7	42155.0	90.7	1784.2	32.7	89.3	1986.0	33.0
50	88.3	40195.0	91.3	1602.0	32.9	90.2	1788.8	33.2

Fixed Fco=2 x 0.00027778[mol/sec]								
	PFR		MR-co			MR-counter		
W/F	X	CO(ppm)	X	CO(ppm)	Re	X	CO(ppm)	Re
10	78.4	76774.0	79.9	3337.2	17.5	78.9	3462.0	17.4
20	84.4	54271.0	86.3	2330.5	17.8	85.4	2433.7	17.8
30	86.7	45999.0	88.7	1891.9	18.0	88.0	1983.2	18.0
40	87.7	42155.0	89.9	1642.3	18.1	89.2	1725.5	18.1
50	88.3	40195.0	90.5	40195.0	18.2	90.0	1558.4	18.3

Fixed Fco=3 x 0.00027778[mol/sec]								
	PFR		MR-co			MR-counter		
W/F	X	CO(ppm)	X	CO(ppm)	Re	X	CO(ppm)	Re
10	78.4	76774.0	79.6	3196.5	12.2	79.0	3272.9	12.1

4.3. *Experimental Verification of Mathematical Model*

- CO conversions vs W/F at 250°C for the feed specified above are presented in Figure 4. Also shown in the figure is the CO conversion based upon the thermodynamic calculation. Permeances for each component were experimentally determined: 1.12, 0.066, 0.163, 1.55 $m^3/m^2/hr/bar$ for H_2, CO, CO_2 and H_2O respectively. With these physical and rate parameters, the CO conversion vs W/F predicted by the mathematical model developed in this study is presented in Figure 4. The MR shows about 10% enhancement over the PFR at this operating condition.

- About 90 and 91% conversion were obtained at W/F= 350 and 400 respectively. These experimental results correlate well with the prediction shown in Figure 4. Additional experimental data will be generated by the end of Year II, particularly in the range of W/F=50 to 200, where the CO conversion is more sensitive to the change of W/F.

T = 250°C; P_{feed} = 3 bar; P_{perm} = 1 bar
Feed Composition: H_2:H_2O:CO:CO_2 = 4:1.1:1:0.01
Permeance [$m^3/m^2/hr/bar$]: H_2: 1.12, CO: 0.066, CO_2: 0.163, H_2O: 1.55

- - - Membrane Reactor: Simulation - - - Plug Flow Reactor: Simulation
── Equilibrium Conversion   ◆ MR Experimental Results
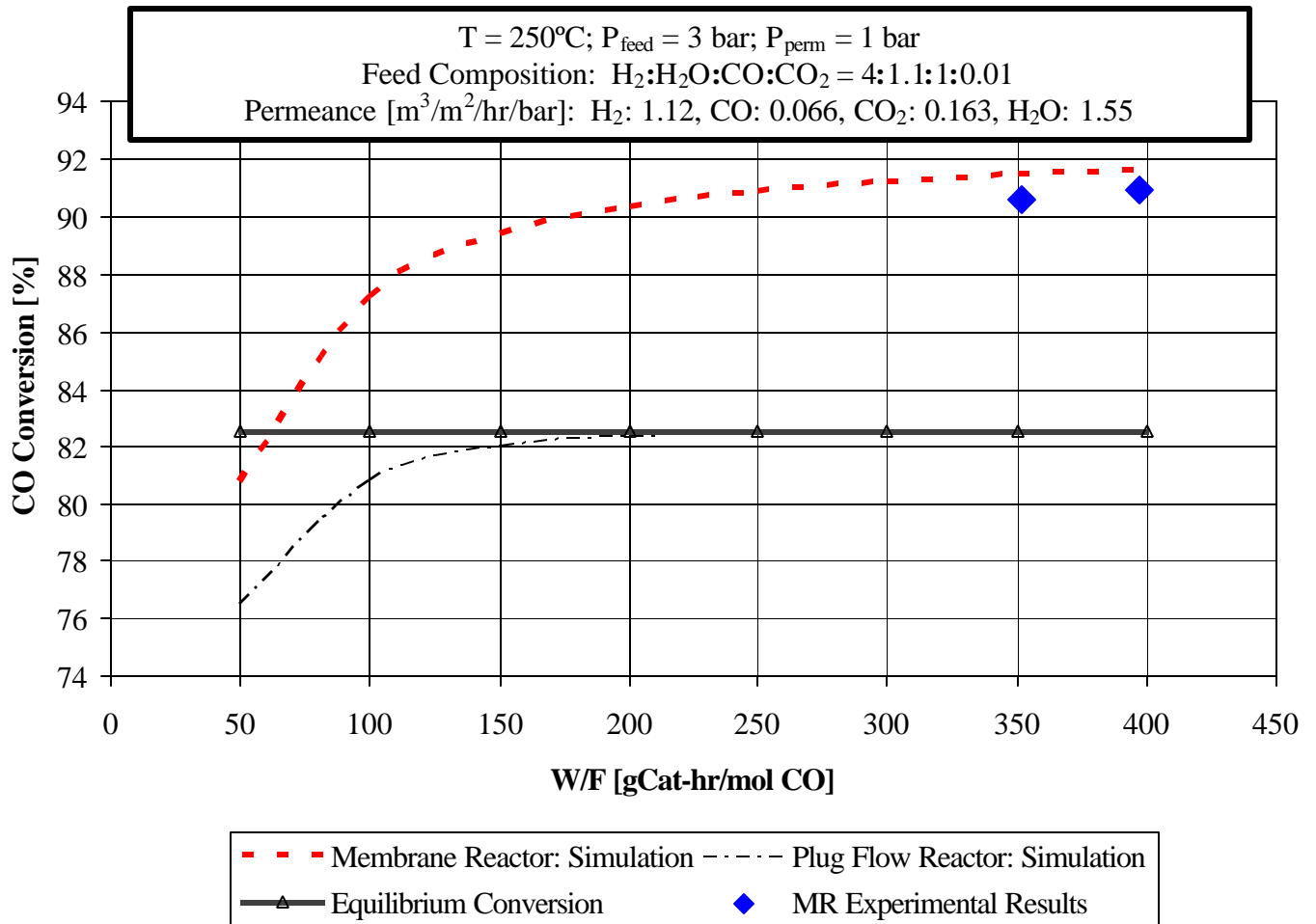
**Figure 4 LTS-WGS USING OUR CMS MEMBRANES AS MR:
Experimental vs Simulation Results**

4.4.   *Temperature Rise and Thermal Management of Proposed Single Stage LTS.*

The exothermic WGS reaction could cause the reactor temperature to rise significantly. To protect the catalyst, an effective thermal management is essential. In the past, the WGS reaction was primarily implemented in the steam reformed stream containing 7 to 10% CO. Thus the temperature rise is not as severe as the WGS for the coal gasifier off-gas, which contains >30% CO.   To accomplish the process intensification objective, instead of using the conventional multiple inter-stage cooler, we have developed an elegant solution to integrate the thermal management into the membrane reactor. An innovative membrane was also developed to accomplish this objective. Due to the proprietary nature of this innovative thermal management approach, no detailed discussion is made here.

4.5.   *Full Scale Membrane and Module Production*

Quantities Produced and On-Spec Ratio…A total of 98 membrane tubes have been produced thus far. We set our spec at a H_2 permeance of >0.35 m^3/m^2/hr and H_2/N_2 selectivity of >50 selectivity at 120ºC. This would translate into a H_2 permeance of >0.5 m^3/m^2/hr/bar and H_2/N_2 selectivity of >75 at the target operating temperature of 250ºC. About 23 out of 98 tubes failed to meet this spec during the first production trial., which leads to >75% on-spec ratio. Please refer to Figure 5 and Table 3 for details.

Full-Scale Module Fabrication… One of the major challenges for ceramic based membranes is its scale up potential. During this reporting period, we have come out with a flexible design, which allows us to fabricate membrane modules with >30 m^2/module without using exotic engineering or materials. This would qualify the ceramic membrane and module for mega-scale applications, such as the proposed application, which usually requires several hundred square meters. With the availability of our innovative module design, ceramic membranes no longer suffer this scale-up disadvantage. Due to the proprietary nature of the design, no details are disclosed here.

Table 4 Characterization of Full-scale Hydrogen Selective Membrane (30"L) produced during this period

| Tube #	Temp [C]	Permeance [m3/m2/hr/bar]		Selectivity		Fail to meet Spec.*
		He	H2	He/N2	H2/N2	
113	120	0.188	0.524	19	53	
114	120	0.306	0.765	32	80	
128	120	0.753	1.390	39	72	
129	120	0.382	0.974	20	51	
130	120	0.278	0.649	42	98	
132	120	0.523	1.068	47	96	
135	120	0.899	2.055	35	80	
137	120	0.454	0.856	87	164	
140	120	0.303	0.598	73	144	
141	120	0.279	0.728	59	154	
143	120	0.557	1.346	24	58	
145	120	0.293	0.760	27	70	
147	120	0.271	0.690	33	84	
148	120	0.548	1.370	34	85	
153	120	0.319	0.775	28	68	
156	120	0.220	0.436	88	175	
163	120	0.244	0.397	56	91	
164	120	0.204	0.345	28	47	x
168	120	0.132	0.157	43	51	x
169	120	0.177	0.253	150	214	x
171	120	0.118	0.146	38	47	x
175	120	0.225	0.500	68	152	
177	120	0.278	0.666	31	73	
178	120	0.259	0.604	21	49	x
180	120	0.684	1.683	28	70	
182	120	0.413	0.897	19	40	
183	120	0.203	0.371	178	324	
184	120	0.306	0.638	73	151	
185	120	0.246	0.604	30	74	
187	120	0.142	0.266	25	46	x
188	120	0.544	1.265	28	64	
190	120	0.399	0.977	44	109	
196	120	0.370	0.763	79	163	
197	120	0.204	0.353	237	409	
198	120	0.679	1.531	25	56	
200	120	0.678	1.356	30	60	
201	120	0.147	0.254	307	532	x
202	120	0.699	1.625	18	42	x
203	120	0.318	0.641	112	225	
204	120	0.170	0.308	119	215	x
205	120	0.323	0.690	30	64	
206	120	0.416	0.707	59	100	
207	120	0.425	0.773	54	99	
208	120	0.241	0.444	31	58	
210	120	0.310	0.637	91	187	
211	120	0.302	0.659	73	160	
214	120	0.297	0.523	214	377	
215	120	0.232	0.355	75	114	
216	120	0.239	0.349	122	178	
218	120	0.253	0.389	150	230	
219	120	0.234	0.347	41	61	
220	120	0.203	0.285	155	217	x
221	120	0.236	0.359	57	86	
223	120	0.246	0.480	24	46	
226	120	0.151	0.282	43	80	x
227	120	0.200	0.320	178	285	x
228	120	0.367	0.697	26	50	
229	120	0.218	0.321	125	183	
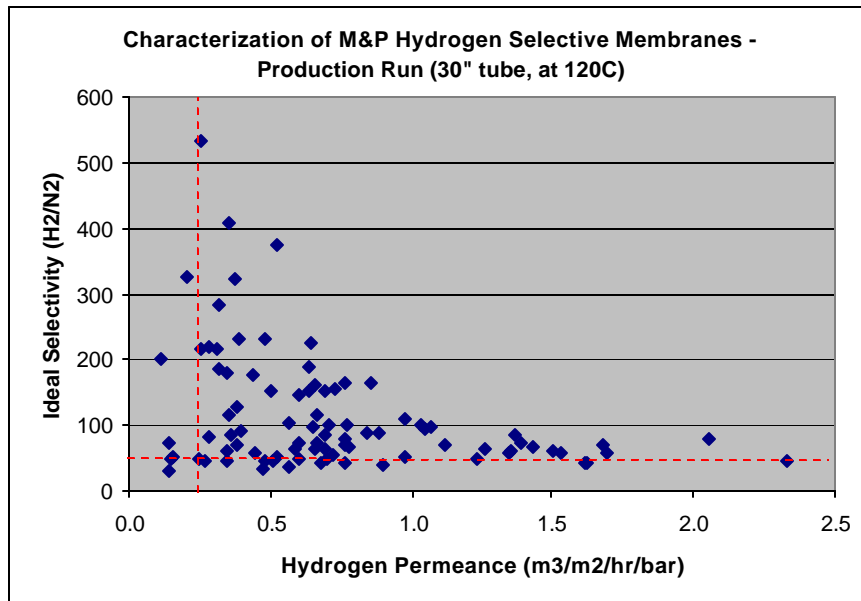
Figure 5. H$_2$ permeance vs. selectivity of full scale membrane tubes prepared during this period.

4.6.   Simulation of WGS Under Field Operating Condition

Conversion under Adequate Permeate Sweep... 88 - 98% CO conversion can be achieved with the MR in comparison with 82 - 89% by the conventional packed bed using a sweep rate of 10 to 40% (sweep ratio of 0.1 to 0.4) of the feed. The conversion vs W/F with the sweep ratio as a parameter is presented in Figure 6. The sweep ratio of 0.3 appears sufficient.

MR vs PFR under Field Operating Condition... 96% CO conversion and <2,000 ppm CO can be produced with the proposed MR vs ~88% conversion and 60,000 ppm CO for the packed bed. The advantage of the membrane performance was enhanced as a result of the increase in the feed pressure and the hydrogen permeance and selectivity used here. The significant improvement in CO conversion and, more importantly, about 30 times reduction in CO contaminant level reinforce the advantage of the membrane reactor for WGS under a field operating condition with our state-of-the-art membrane. Optimization will begin once the experimental verification is completed by the end of Yr II.

Simulation of Test Unit at PFDU... Presently, this mathematical model has been utilized to simulate the WGS operation at PFDU (Wilsonville, AL). Several operating conditions have been provided by PFDU engineers for us to simulate the hydrogen separation potential. Our simulation results were then used to estimate its potential improvement in WGS by PFDU personnel using its ASPEN model. The potential improvement of using

our membranes and membrane reactors will be documented in the 2nd semiannual report of Yr II. A field test is planned in Yr III using the membrane module provided by Media and Process Technology Inc.

*Membrane Performance Stability in Presence of Concentrated H₂S...*The field test results generated at the refinery pilot test facility are summarized in Figure 7. At 220°C and 10 bar, a stable hydrogen permeance of 1.1 $m^3/m^2/hr/bar$ was obtained throughout the test period of about 120 hrs. Hydrogen purity was enriched from ~90% to 99.9% with the hydrogen recovery ratio of 85 to 92%. In addition, the H_2S concentration was reduced from 5.2% in the feed to =0.16% in the permeate. More importantly, no membrane permeance degradation was observed under this concentrated H_2S environment.

*Membrane Regeneration after Challenge Test...*The aggressive "dead-head" (no reject flow) challenge test reduced the permeance substantially; however, our regeneration restored the original permeance as presented in Table 4. Hydrogen permeance of 1.27 $m^3/m^2/hr/bar$ and the selectivity of ~75 for hydrogen over nitrogen at 220°C were obtained before the challenge test. The dead head challenge test was conducted for 17 hours so that the contaminant levels far exceeded those in the standard run, including >>30% H_2S and heavy hydrocarbons. As a result, the membrane was poisoned and its permeance was reduced by ~50% to 0.62 $m^3/m^2/hr/bar$. However, this permeance loss was restored via our proprietary regeneration technique to nearly the original level, i.e., 1.26 $m^3/m^2/hr/bar$ and the selectivity of 67. Based upon the results from the poison study in the field and its regeneration, we believe that our CMS membrane can be regenerated in case the membrane is accidentally poisoned.
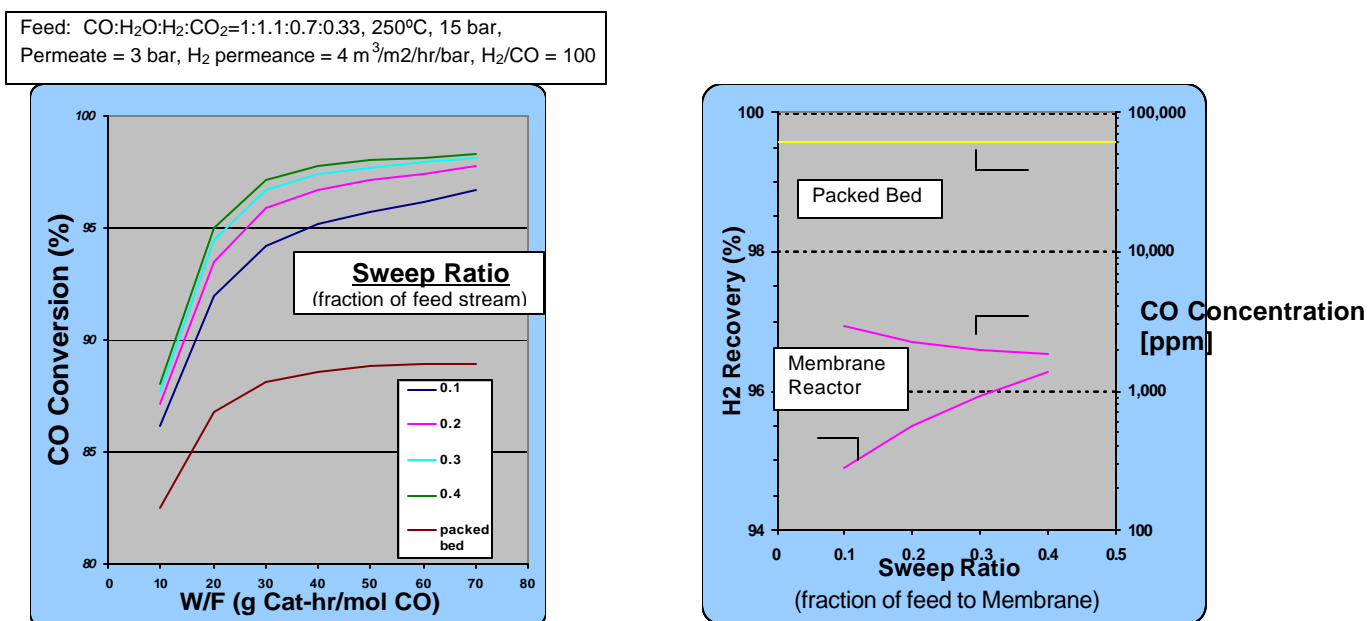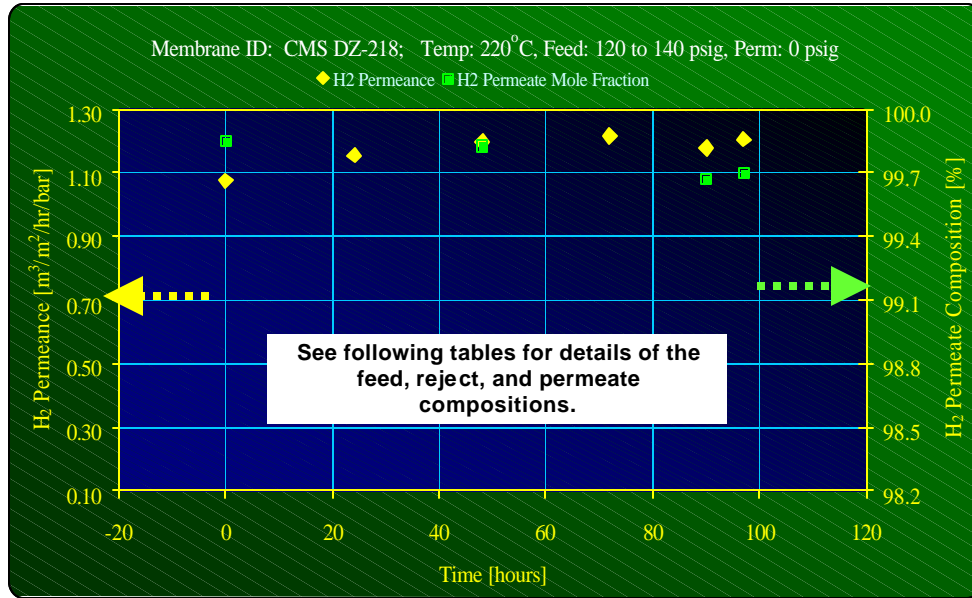
Feed: $CO:H_2O:H_2:CO_2$=1:1.1:0.7:0.33, 250°C, 15 bar, Permeate = 3 bar, H_2 permeance = 4 m³/m2/hr/bar, H_2/CO = 100

Figure 6. **Effect of permeate sweep gas rate on CO conversion with our proposed membrane reactor**

17

Membrane ID: CMS DZ-218; Temp: 220°C, Feed: 120 to 140 psig, Perm: 0 psig

◆ H2 Permeance ■ H2 Permeate Mole Fraction

During this 100 hr field test, our membrane shows excellent H_2 permeance and selectivity in the presence of H_2S, ammonia and hydrocarbons.

At time = 3 hours					At time = 100 hours			
Gas	Composition [%]			H_2/Slow Selectivity	Gas	Composition [%]			H_2/Slow Selectivity
	Feed	Reject	Permeate			Feed	Reject	Permeate	
H_2S	5.2	32.0	0.03	163	H_2S	4.8	24.5	0.16	74
H_2	89.9	38.9	99.88	1	H_2	90.8	50.6	99.70	1
C_1	2.1	12.2	0.08	123	C_1	1.9	9.9	0.06	123
C_2	0.88	5.4	0.01	~600	C_2	0.81	4.2	0.01	~600
C_3+	1.88	11.6	ND	>1,000	C_3+	1.66	10.7	ND	>1,000
Stage Cut			85%		Stage Cut			80%	
H_2 Recovery			92%		H_2 Recovery			85%	

Figure 7   **Gas Stream Compositions and Stage Cut and H_2 Recovery for the VGO Hydrocracker Pilot Test**

Table 5   Degradation of the carbon molecular sieve membrane challenged by the dead-end operation and the restoration of the original permeance via regeneration.

Membrane Regeneration

Pure Component Permeance and Selectivity

Test Conditions: 220ºC @ ~120 psig

Test Phase	H_2 [$m^3/m^2/hr/bar$]	H_2/N_2 [-]
Before Hydrocracker Testing	1.27	75
After Hydrocracker Testing	1.22	ND
After Dead Head Hydrocracker Challenge Test >> ~17 hrs w/NO Reject Flow (100% Stage Cut) >> Permeate flow falls from ~450 to ~3 cc/min	0.62	53
After Regeneration	1.26	67

$$CO + H_2O \Leftrightarrow CO_2 + H_2 \tag{1}$$

$$r = k \frac{P_{CO} P_{H_2O}^{1.4}}{P_{H_2}^{0.9} P_{CO_2}^{0.7}} (1 - \boldsymbol{b}) \frac{1}{P_t^{0.4}} \tag{2}$$

$$\boldsymbol{b} = \frac{P_{CO_2} P_{H_2}}{K_e P_{H_2O} P_{CO}} \tag{3}$$

$$k = k_o \cdot \exp(-\frac{E_a}{RT}) \tag{4}$$

k_o is the preexponential factor, E_a is the apparent activation energy, P_j is the partial pressure of component j, P_t is the total pressure, $\boldsymbol{b}$ is the approach to equilibrium and K_g is the equilibrium constant for the water-gas shift reaction.

Mass transfer through the porous membrane is described by the following empirical equation:

$$F_j = U_j (P_j^F - P_j^P) \tag{5}$$

where F_j is the molar flux (mol/m^2·s), P_j^F the partial pressure of component j on the membrane feed side (bar), P_j^P the partial pressure of component j on the membrane permeate side (bar), and U_j the membrane permeance for component j (mol/m^2·bar·s).

The mass balance on the feed side of the reactor packed with water gas shift reaction catalyst is described by the following equations for CO_2, CO, H_2, H_2O and an inert species (potentially used as a sweep gas or a blanketing agent; for catalytic water gas shift reaction, a practical sweep gas would be either steam or hydrogen, however):

Feed side: $\dfrac{\partial n_j^F}{\partial z} = -\boldsymbol{a}_m U_j (P_j^F - P_j^P) + \boldsymbol{u}_j A_c r^F \tag{6}$

Permeate side: $\dfrac{\partial n_j^P}{\partial z} = \boldsymbol{a}_m U_j (P_j^F - P_j^P) \tag{7}$

$j=1,2....n$

at $z = 0$, $n_j = n_{jo} \tag{8}$

In eq. 6 and 7, n_j^F is the molar flow rate (mol/s) for species j on the feed side. n_j^P is the molar flow rate (mol/s) for species j on the permeate side, z is the reactor length variable (m), A_c the cross-sectional area available to flow for the reactor feed side (m^2), $\boldsymbol{a}_m$ the

inner circumference of the membrane (m), u_i the stoichiometric coefficient of component j and r^F the reaction rate expression.

The pressure drop in a packed bed can be calculated using the Ergun equation:

$$-\frac{dP^F}{dz} = 10^{-6} \frac{f \ (G^F)^2}{g_c d_P \mathbf{r}^F} \tag{9}$$

$$\text{at } z = 0, \quad P^F = P_0^F \tag{10}$$

$$f = \left(\frac{1-\mathbf{e}_v}{(\mathbf{e}_v)^3}\right)\left(1.75 + \frac{150(1-\mathbf{e}_v)}{N_{Re}^F}\right) \tag{11}$$

$$N_{Re}^F < 500(1-\mathbf{e}_v) \tag{12}$$

$$N_{Re}^F \equiv d_P G^F / \mathbf{m}^F \tag{13}$$

where P^F is the feed-side pressure (bar), P_0^F the inlet feed-side pressure, $\mathbf{m}^F$ the viscosity (Pa·s), d_P the particle diameter in the feed side (m), $G^F = \mathbf{r}^F u^F$ the superficial mass flow velocity in the feed side (kg/m²·s), u^F the average velocity of the fluid, $\mathbf{r}^F$ the average density of the fluid (kg/m³), and g_c the gravity conversion factor equal to 1 in SI units.

The reactor conversion (based on CO, which is typically the limiting reagent) is defined by the following equation:

$$X_{CO} = \frac{n_{CO_0}^F - (n_{CO_{ex}}^F + n_{CO_{ex}}^P)}{n_{CO_0}^F} \tag{14}$$

where $n_{CO_0}^F$ is the inlet molar flow rate of CO and $n_{CO_{ex}}^F$ and $n_{CO_{ex}}^P$ are the CO molar flow rates at the exit of the reactor feed and permeate sides correspondingly (mol/s). The yield of product hydrogen, defined as the fraction of moles of CO fed into the reactor that have reacted to produce hydrogen, is given by the following equation:

$$Y_{H_2} = \frac{(n_{H_{2,ex}}^F - n_{H_{2,0}}^F) + (n_{H_{2,ex}}^P - n_{H_{2,0}}^P)}{n_{CO_0}^F} \tag{15}$$

where $n_{H_{2,ex}}^F$ and $n_{H_{2,ex}}^P$ are the hydrogen molar flow rates at the exit of respectively the reactor feed and permeate sides and $n_{H_{2,0}}^F$ and $n_{H_{2,0}}^P$ the H_2 molar flow rates potentially present at the inlet of the reactor feed and permeate sides (mol/s). $Y_{H2} = 1$ when all of the CO has reacted completely to produce CO_2 and H_2.

Equations 1.7-1.10 can be written by defining the following variables and groups:

$$n_o^F = \sum_j n_{jo}^F \; ; \; n_o^P = \sum_j n_{jo}^P \; ; n^F = n_o^F \sum_j x_j^F \; ; n^P = n_o^P \sum_j x_j^P$$

$$x_j^F \equiv \frac{n_j^F}{n_o^F} \; ; x_j^P \equiv \frac{n_j^P}{n_o^P}$$

$$y_j^F = \frac{n_j^F}{n^F} = \frac{x_j^F}{\sum_j x_j^F} \; ; \; y_j^P = \frac{n_j^P}{n^P} = \frac{x_j^P}{\sum_j x_j^P}$$

$$\Psi^F \equiv \frac{P^F}{P_0^F} \; ; \; \Psi^P \equiv \frac{P^P}{P_0^P} \; ; \; \boldsymbol{x} \equiv \frac{z}{L} \; ; \; Pe_j^F \equiv \frac{n_0^F}{\boldsymbol{a}_m U_j P_o^F L} \; ; \; Da \equiv \frac{A_C L}{n_o^F}$$

$$P_j^F = y_j^F \cdot P^F = \frac{x_j^F}{\sum_j x_j^F} P_o^F \Psi^F \; ; \; P_j^P = y_j^P \cdot P^P = \frac{x_j^P}{\sum_j x_j^P} P_o^P \Psi^P$$

$$MW_{ave}^F = \frac{\sum_j x_j^F MW_j}{\sum_j x_j^F}$$

$$\boldsymbol{r}^F = \frac{P^F MW_{ave}^F}{RT} = \frac{P_o^F \Psi^F \sum_j x_j^F MW_j}{RT \sum_j x_j^F}$$

$$u^F = \frac{Q^F}{A^F} = \frac{n^F RT}{P^F A^F} = \frac{n_o^F RT \sum_j x_j^F}{P_o^F \Psi^F A^F}$$

$$G^F = \boldsymbol{r}^F u^F = \frac{n_o^F \sum_j (x_j^F MW_j)}{A^F} \tag{16}$$

The equations equivalent to eqs 1.7-1.10 are

$$-\frac{d\Psi^F}{d\boldsymbol{x}} = \frac{L}{P_o^F} \frac{f^F (G_m^F)^2}{g_c d_P^F \boldsymbol{r}^F} \tag{17}$$

Feed side: $\quad \dfrac{dx_j^F}{d\boldsymbol{x}} = -\dfrac{1}{Pe_j^F} \left(\dfrac{x_j^F}{\sum_j x_j^F} \Psi^F - \dfrac{x_j^P}{\sum_j x_j^P} \Psi^P \right) + \boldsymbol{u}_j Da \cdot r^F \tag{18}$

Permeate side: $\dfrac{dx_j^P}{d\boldsymbol{x}} = \dfrac{1}{Pe_j^F} \left(\dfrac{x_j^F}{\sum_j x_j^F} \Psi^F - \dfrac{x_j^P}{\sum_j x_j^P} \Psi^P \right) \tag{19}$

$$\text{at } \boldsymbol{x} = 0, \quad \Psi^F = 1, \quad \Psi^P = 1 \tag{20}$$

Appendix II: Material Balance of the Mathematical Mode l Developed in this Study.

Water gas shift reaction is as follows;

$$CO + H_2O \leftrightarrow CO_2 + H_2$$
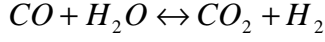
Mass balance for component CO along the reactor for counter-current flow system is as follows,

$$\frac{d(n_{CO}^F)}{dz} = \boldsymbol{p}(R_o^2 - R_i^2) \cdot r_{CO} - 2\boldsymbol{p} \cdot R_i \cdot K_{CO}(p_{CO}^F - p_{CO}^P) \qquad (1) - \text{Feed side}$$

$$\frac{d(n_{CO}^P)}{dz} = -2\boldsymbol{p} \cdot R_i \cdot K_{CO}(p_{CO}^F - p_{CO}^P) \qquad (2) - \text{Permeate side}$$

From (1) and (2) we obtain

$$\frac{d(n_{CO}^F - n_{CO}^P)}{dz} = A_C \cdot r_{CO} \qquad (3)$$

Where,

$$A_c \equiv \boldsymbol{p}(R_o^2 - R_i^2)$$

Similarly, for component H_2O, CO_2 and H_2

$$\frac{d(n_{H_2O}^F - n_{H_2O}^P)}{dz} = A_C \cdot r_{H_2O} = A_C \cdot r_{CO} \qquad (4)$$

$$\frac{d(n_{CO_2}^F - n_{CO_2}^P)}{dz} = A_C \cdot r_{CO_2} = -A_C \cdot r_{CO} \qquad (5)$$

$$\frac{d(n_{H_2}^F - n_{H_2}^P)}{dz} = A_C \cdot r_{H_2} = -A_C \cdot r_{CO} \qquad (6)$$

Add (3) and (5), we can get an equation with respect to C

$$r_{CO} + r_{CO_2} = A_C \cdot \frac{d(n_{CO}^F + n_{CO_2}^F - n_{CO}^P - n_{CO_2}^P)}{dz} = 0 \qquad (7)$$

$$n_{CO}^F + n_{CO_2}^F - n_{CO}^P - n_{CO_2}^P = const. \qquad (8)$$

Similarly, with respect to H

$$r_{H_2O} + r_{H_2} = 0 \tag{9}$$

$$n_{H_2O}^F + n_{H_2}^F - n_{H_2O}^P - n_{H_2}^P = const. \tag{10}$$

And O

$$r_{CO} + r_{H_2O} + 2r_{CO_2} = 0 \tag{11}$$

$$n_{CO}^F + n_{H_2O}^F + 2n_{CO_2}^F - n_{CO}^P - n_{H_2O}^P - 2n_{CO_2}^P = const. \tag{12}$$

Of course we don't need to make special forms such as (7), (9) and (11) because many expressions can be created. For example,

(3)+ (6) = 0
(4)+ (5) = 0

The following 5 graphs were obtained under the condition which is
Counter-current flow system
T = 250 ^{o}C, P$_F$ = 3 atm, P$_P$ = 1 atm, W/F$_{CO}$ = 12.9(g-cat*hr/gmol CO)
Rich's base case

Note that the green lines in the following graphs are exactly same. (Figure 1, 2, 3 and 4)
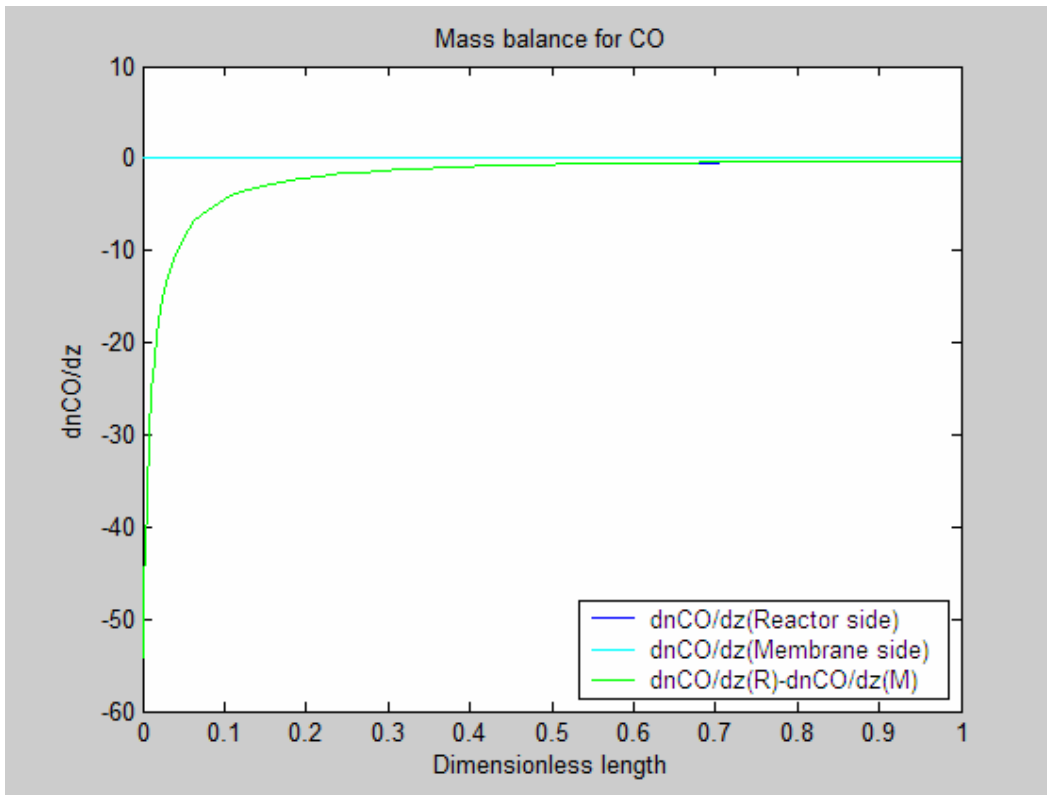
Figure 1 $\dfrac{dn_{CO}^{F}}{dz}, \dfrac{dn_{CO}^{P}}{dz}, \dfrac{dn_{CO}^{F} - dn_{CO}^{P}}{dz}$
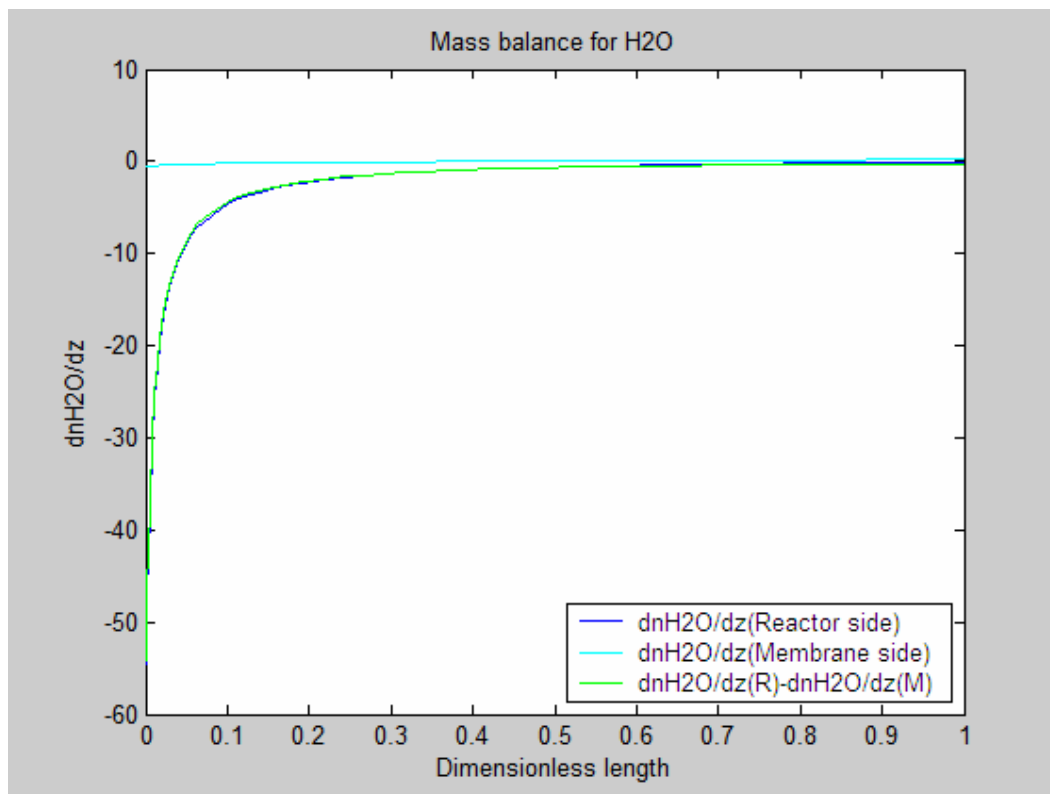
Figure 2 $\dfrac{dn_{H_2O}^{F}}{dz}, \dfrac{dn_{H_2O}^{P}}{dz}, \dfrac{dn_{H_2O}^{F} - dn_{H_2O}^{P}}{dz}$
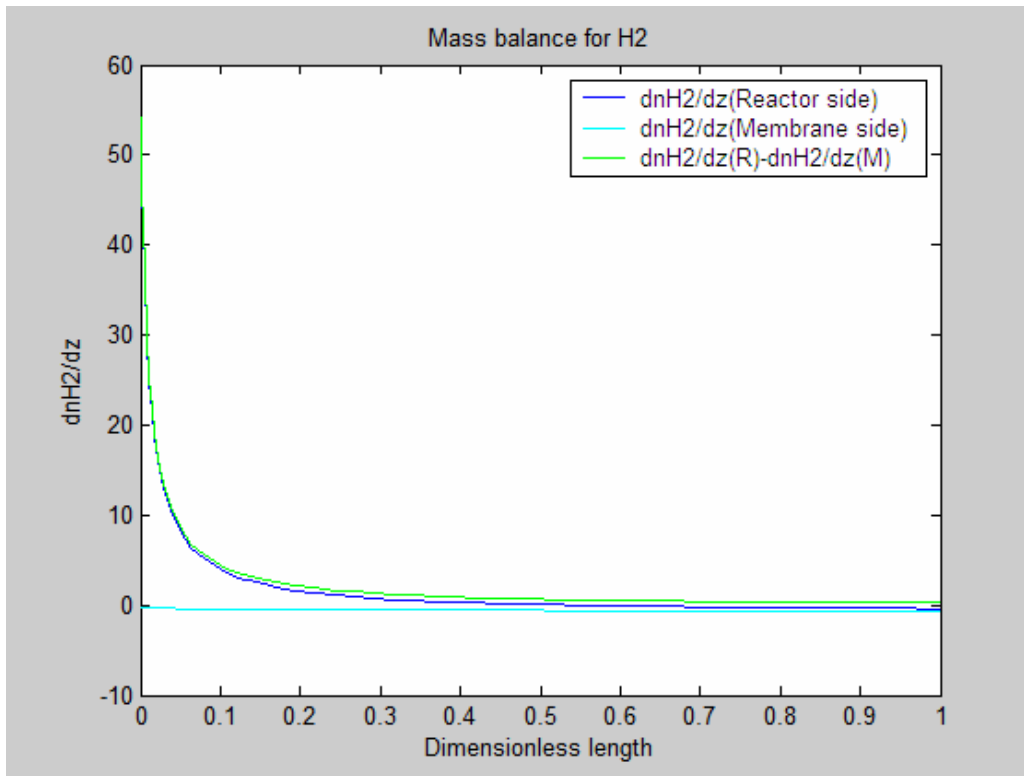
Figure 3 $\dfrac{dn_{H_2}^F}{dz}, \dfrac{dn_{H_2}^P}{dz}, \dfrac{dn_{H_2}^F - dn_{H_2}^P}{dz}$
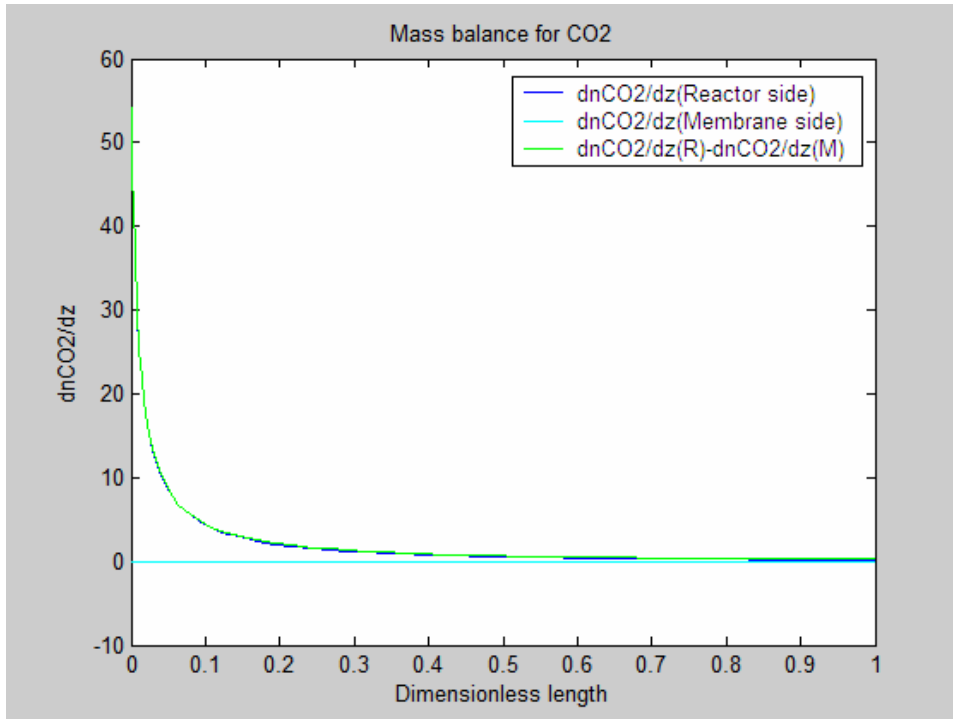
Figure 4 $\dfrac{dn_{CO_2}^F}{dz}, \dfrac{dn_{CO_2}^P}{dz}, \dfrac{dn_{CO_2}^F - dn_{CO_2}^P}{dz}$
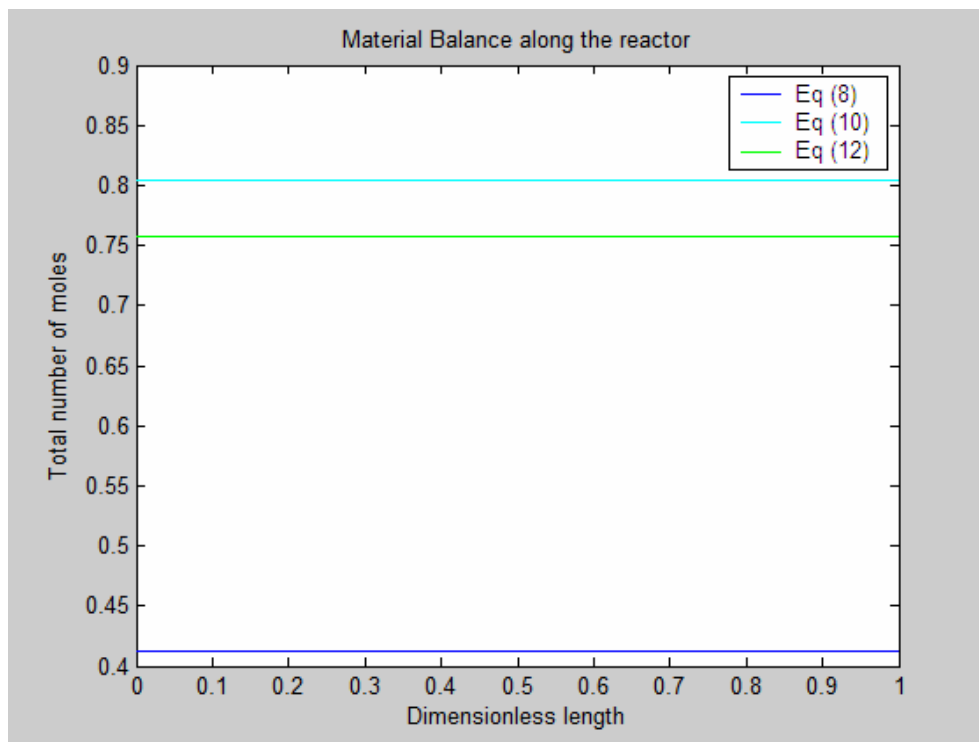
Figure 5 Eq. (8), (10) and (12)

In case of the co-current system, the sign for the permeate side must be changed. For example, if we get the mass balance for CO again, it goes

$$\frac{d(n_{CO}^F)}{dz} = A_C \cdot r_{CO} - 2\boldsymbol{p} \cdot R_i \cdot K_{CO}(p_{CO}^F - p_{CO}^P) \qquad (13) - \text{Feed side}$$

$$\frac{d(n_{CO}^P)}{dz} = 2\boldsymbol{p} \cdot R_i \cdot K_{CO}(p_{CO}^F - p_{CO}^P) \qquad (14) - \text{Permeate side}$$

From (1) and (2) we obtain

$$\frac{d(n_{CO}^F + n_{CO}^P)}{dz} = A_C \cdot r_{CO} \qquad (15)$$

Similarly, for component H_2O, CO_2 and H_2

$$\frac{d(n_{H_2O}^F + n_{H_2O}^P)}{dz} = A_C \cdot r_{H_2O} = A_C \cdot r_{CO} \qquad (16)$$

$$\frac{d(n_{CO_2}^F + n_{CO_2}^P)}{dz} = A_C \cdot r_{CO_2} = -A_C \cdot r_{CO} \qquad (17)$$

$$\frac{d(n_{H_2}^F + n_{H_2}^P)}{dz} = A_C \cdot r_{H_2} = -A_C \cdot r_{CO} \qquad (18)$$

Add (3) and (5), we can get an equation with respect to C

$$r_{CO} + r_{CO_2} = A_C \cdot \frac{d(n_{CO}^F + n_{CO_2}^F + n_{CO}^P + n_{CO_2}^P)}{dz} = 0 \qquad (19)$$

$$n_{CO}^F + n_{CO_2}^F + n_{CO}^P + n_{CO_2}^P = const. \qquad (20)$$

Similarly, with respect to H

$$r_{H_2O} + r_{H_2} = 0 \qquad (21)$$

$$n_{H_2O}^F + n_{H_2}^F + n_{H_2O}^P + n_{H_2}^P = const. \qquad (22)$$

And O

$$r_{CO} + r_{H_2O} + 2r_{CO_2} = 0 \qquad (23)$$

$$n_{CO}^F + n_{H_2O}^F + 2n_{CO_2}^F + n_{CO}^P + n_{H_2O}^P + 2n_{CO_2}^P = const. \qquad (24)$$

Now, the following 5 graphs were obtained under the same condition described above at co-current flow system.
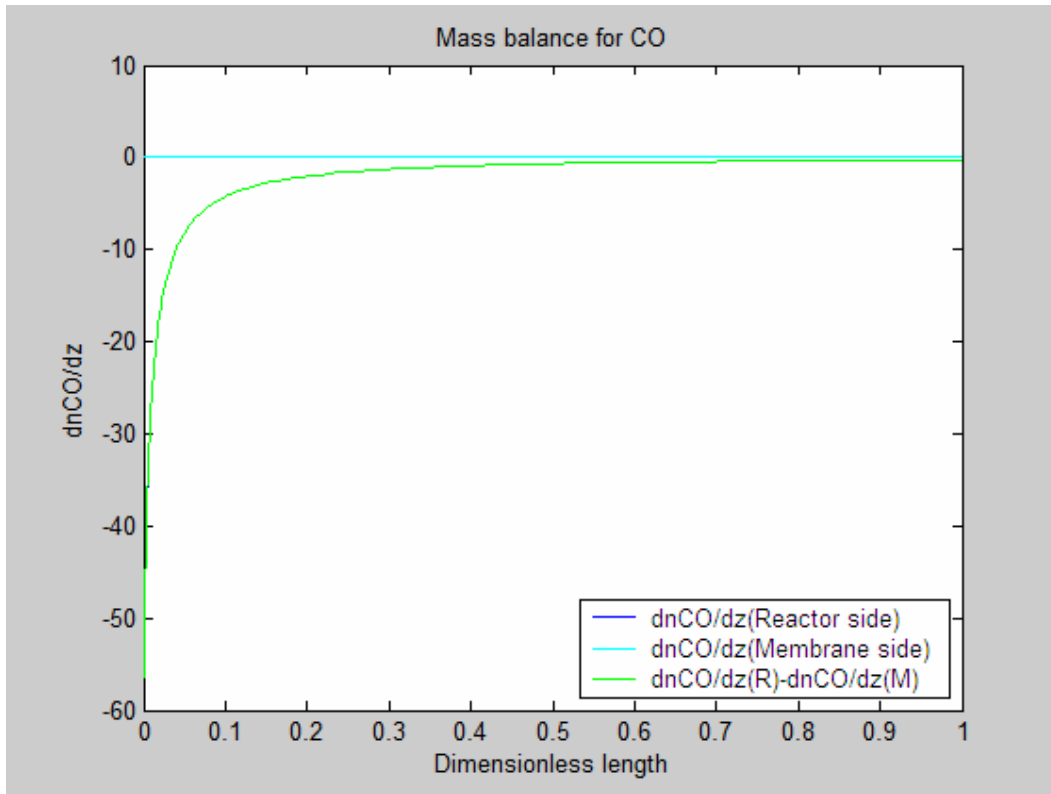

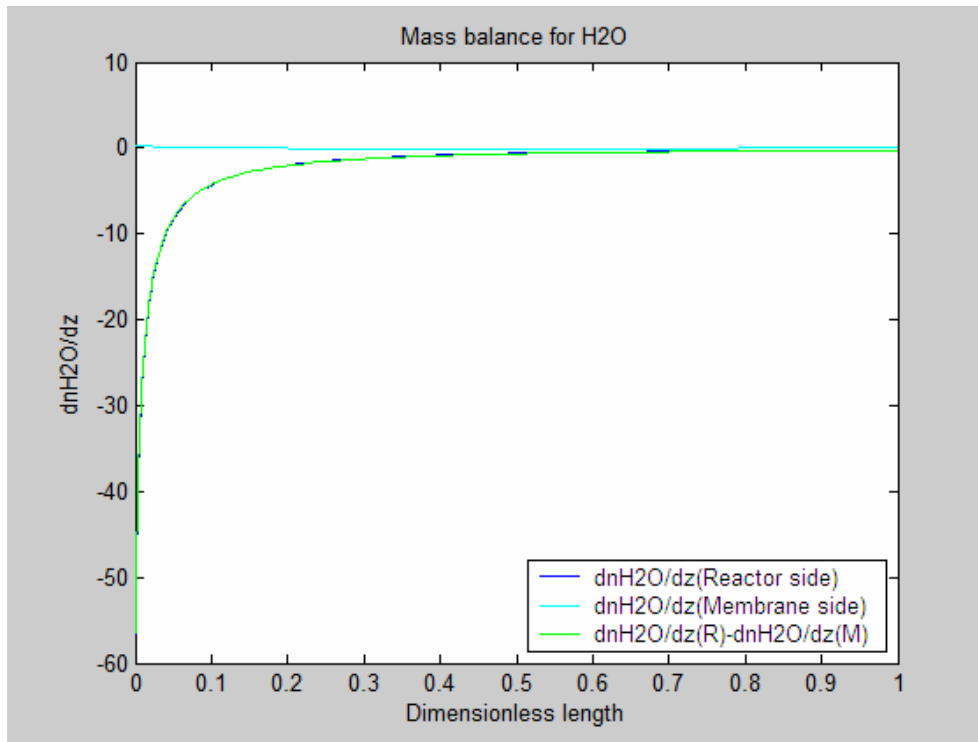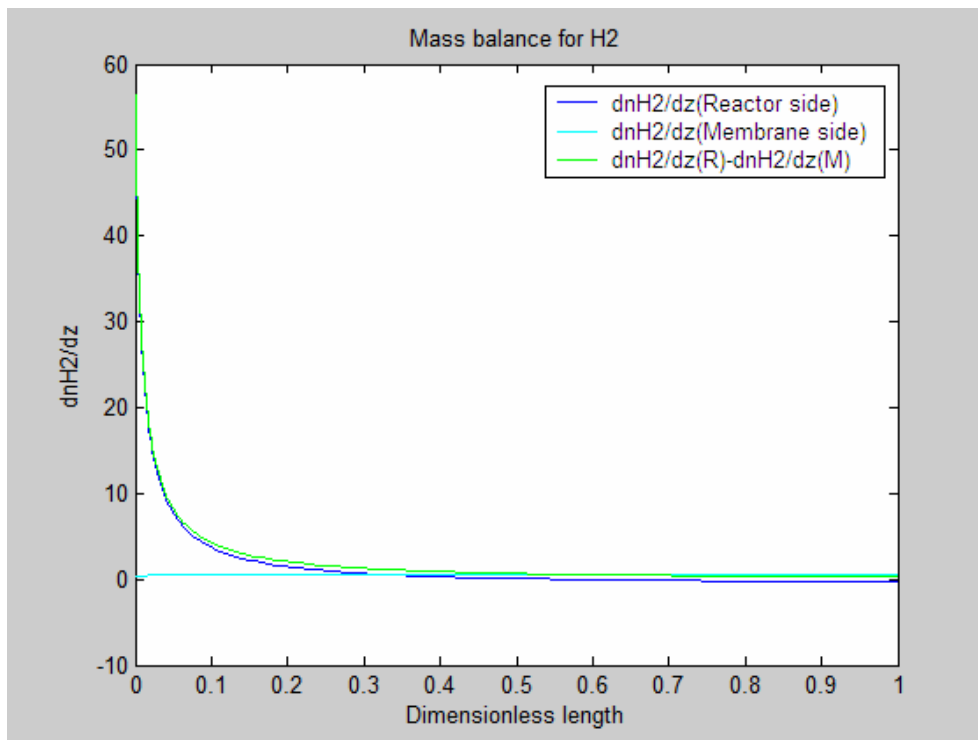Figure 6 $\dfrac{dn_{CO}^F}{dz}, \dfrac{dn_{CO}^P}{dz}, \dfrac{dn_{CO}^F + dn_{CO}^P}{dz}$

Figure 7 $\dfrac{dn^F_{H_2O}}{dz}, \dfrac{dn^P_{H_2O}}{dz}, \dfrac{dn^F_{H_2O} + dn^P_{H_2O}}{dz}$

Figure 8 $\dfrac{dn^F_{H_2}}{dz}, \dfrac{dn^P_{H_2}}{dz}, \dfrac{dn^F_{H_2} + dn^P_{H_2}}{dz}$
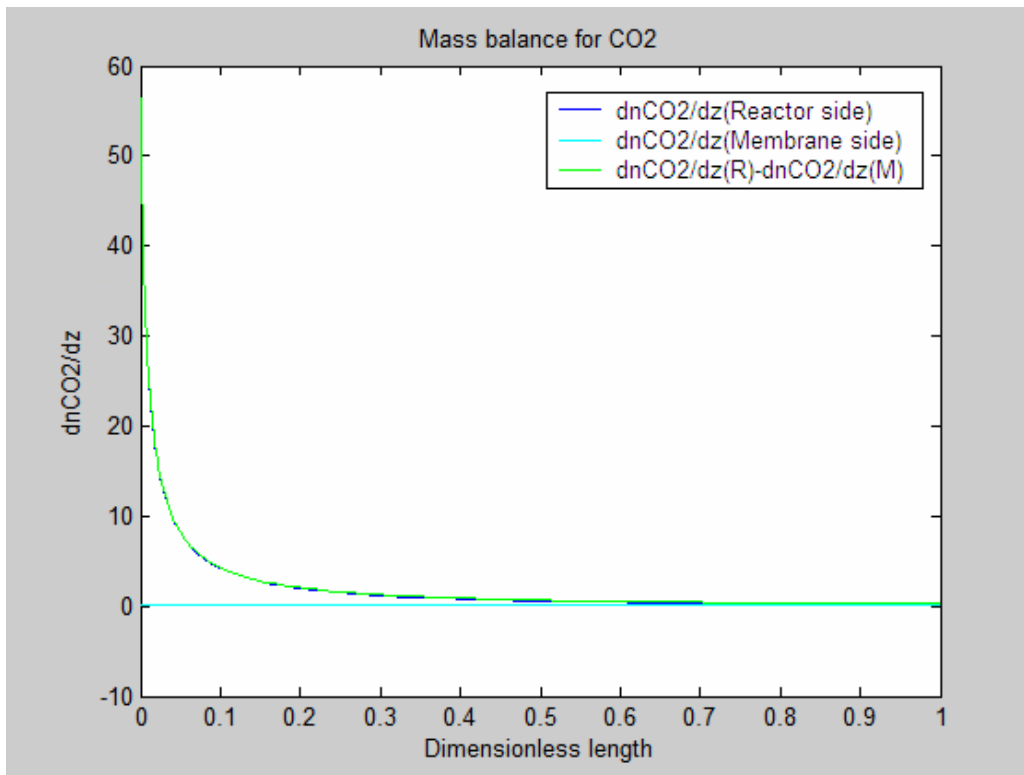
Figure 9 $\dfrac{dn_{CO_2}^F}{dz}, \dfrac{dn_{CO_2}^P}{dz}, \dfrac{dn_{CO_2}^F + dn_{CO_2}^P}{dz}$
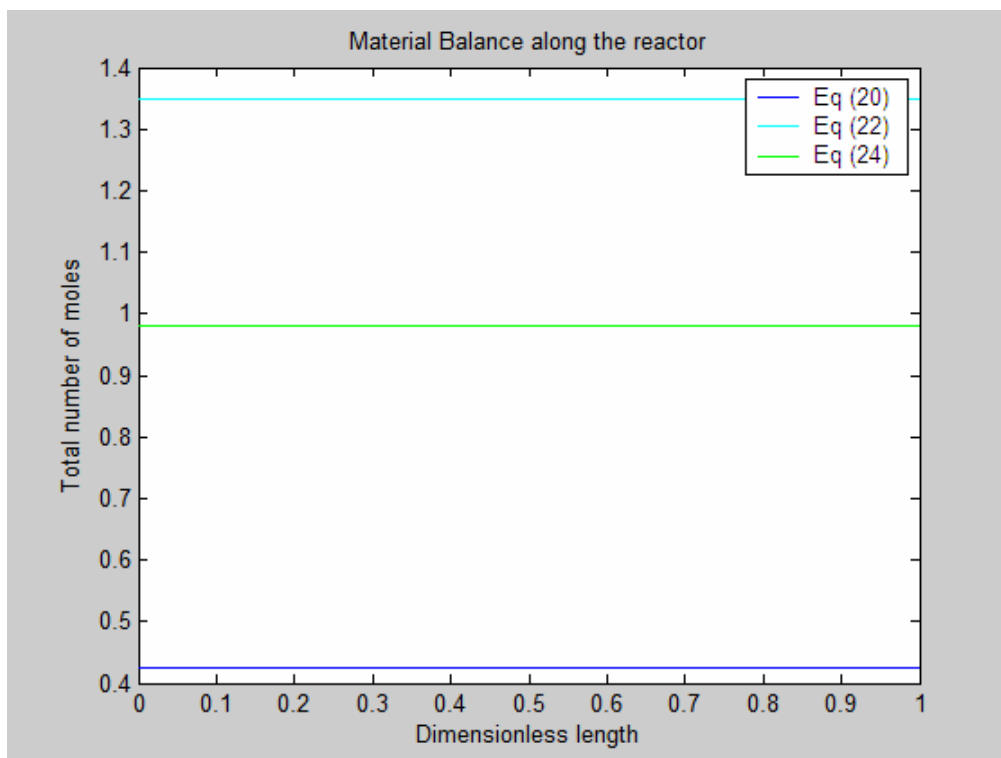

Figure 10 Eq. (20), (22) and (24)

Conclusion:

Key conclusions drawn from the study during this period include:

- Single stage low-temperature-shift water-gas-shift (WGS-LTS) via a membrane reactor (MR) process was studied through both mathematical simulation and experimental verification in this period. Using the kinetic parameters experimentally obtained by us, we are able to validate the mathematical model via the bench-top experimental results.

- Although the thermodynamic conversion of CO could be as high as ~90% in the LTS range, our proposed MR yields a reactor size that is 10 to >55% smaller than the comparable conventional reactor for a CO conversion of 80 to 90%. In addition, the CO contaminant level in the hydrogen produced via MR ranges from 1,000 to 4,000 ppm vs 40,000 to >70,000 ppm via the conventional reactor. The advantages of the reduced WGS reactor size and the reduced CO contaminant level provide an excellent opportunity for intensification of the hydrogen production process by the proposed MR.

- A significant number (i.e., 98) of full-scale membrane tubes have been produced with an on-spec ratio of >76% during this first production trial. In addition, an innovative full-scale membrane module has been designed, which can potentially deliver >20 to 30 m^2/module making it suitable for large-scale applications, such as power generation.

- Our membrane performance and stability were verified in a refinery pilot testing facility on a hydrocracker purge gas. No change in membrane performance was noted over the >100 hrs of testing conducted in the presence of >30% H$_2$S, >5,000 ppm NH$_3$ (estimated), and heavy hydrocarbons on the order of 25%. The high stability of these membranes opens the door for the use of our membrane in the WGS environment with significantly reduced pretreatment burden.

We have also worked on (i) thermal management for the proposed one-stage WGS reactor, and (ii) defining and planning the field test in Year III at the PFDU facility. These results will be reported in the next report.

Literature Cited:

1. C. V. Ovesen, et. al. "A Microkinetic Analysis of the Water-Gas Shift Reaction under Industrial Conditions", *Journal of Catalysis* 158, 170-180 (1996)

List of Acronyms:

LTS: low temperature shift
WGS: water gas shift reaction
MR: membrane reactor
PFR: packed fixed-bed reactor
Ea: activation energy